

ULTRAFINE PALLADIUM NANOPARTICLES SUPPORTED ON THE MFI ZEOLITE FOR METHANE COMBUSTION REACTION

Tao Cai, Ning Wang, Yue Sun*

College of Chemistry and Chemical Engineering, Qingdao University, Qingdao 266071, Shandong, China.

*Corresponding Author: Yue Sun

Abstract: The environmental impact of methane's incomplete combustion underscores the importance of catalytic oxidation, a process in which palladium (Pd) nanoparticles serve as a highly active catalyst despite their tendency to aggregate during synthesis and operation due to inherent high surface energy. Zeolites, as nanoporous materials with ordered micropore structures and excellent thermal stability, are considered ideal supports for stabilizing noble metal nanoparticles. Herein, MFI-type zeolite nanosheets rich in silanol defects were used as supports to prepare finely dispersed Pd nanocatalysts (Pd/SP-S-1 and Pd/SP-ZSM-5) via incipient wetness impregnation. The resulting catalysts exhibited excellent activity toward methane combustion. The T_{90} (temperature for 90% methane conversion) value of Pd/SP-S-1 was 459 °C, which is lower than that of the catalyst supported on conventional S-1 zeolite. Introducing acidity further enhanced the catalytic performance, lowering the T_{90} of Pd/SP-ZSM-5 to 426 °C. Moreover, the acidic zeolite framework improved the stability of Pd nanoparticles. The Pd/SP-ZSM-5 catalyst maintained stable activity for nearly 50 h at 430 °C. This work highlights the potential of zeolite-confined Pd catalysts for methane combustion and provides insights into designing synergistic catalytic systems combining metallic and acidic sites.

Keywords: Pd nanocatalyst; Methane; Catalytic combustion; Zeolite

1 INTRODUCTION

Methane (CH_4) has been extensively utilized as a clean fuel owing to its high energy density, high hydrogen-to-carbon ratio, and relatively low emissions of conventional air pollutants compared with coal- and oil-derived fuels [1]. However, methane is also a potent greenhouse gas, and even trace amounts of unburned methane released during incomplete combustion can cause significant environmental concerns. Catalytic combustion is widely regarded as one of the most effective approaches for the removal of low-concentration methane emissions [2]. Nevertheless, achieving efficient methane oxidation at low temperatures remains a formidable challenge due to the exceptional chemical inertness of methane, which originates from its highly symmetric molecular structure and strong C-H bonds with a bond dissociation energy of approximately 413 kJ mol⁻¹. Among the various catalyst systems investigated, noble-metal-based catalysts have demonstrated the highest activity for methane combustion. Supported palladium (Pd) nanoparticles, in particular, are recognized as the most active catalysts for methane oxidation [3]. Despite their high intrinsic activity, Pd nanoparticles suffer from severe aggregation during synthesis and under reaction conditions as a result of their high surface energy, leading to particle growth, loss of active sites, and rapid catalyst deactivation [4].

Zeolites, featuring well-defined microporous frameworks and outstanding thermal stability, are promising supports for stabilizing noble metal species [5-6]. In industrial catalyst preparation, the impregnation method is widely employed because of its simplicity and scalability; however, this conventional approach often leads to uncontrolled metal nucleation and particle growth, resulting in poor metal dispersion and limited catalyst durability [7]. Therefore, developing a simple and effective impregnation-based strategy to construct highly dispersed and stable metal catalysts remains a key challenge in heterogeneous catalysis. In recent years, two-dimensional nanosheet zeolites have emerged as attractive catalyst supports due to their unique structural characteristics [8]. Compared with conventional three-dimensional zeolites, nanosheet architectures possess higher external surface areas and shortened diffusion pathways, which significantly enhance mass transport and catalytic efficiency [9]. Moreover, the abundant surface silanol defects present on nanosheet zeolites provide favorable anchoring sites for metal precursors, enabling uniform metal dispersion and the formation of ultrafine metal nanoparticles [10]. The integration of highly dispersed metal active centers with mass-transfer-enhanced nanosheet zeolite supports thus offers a promising platform for the design of advanced catalysts with high activity, excellent stability, and improved accessibility for methane oxidation.

Defect-rich MFI-type zeolite nanosheets were utilized as supports to fabricate highly dispersed Pd nanocatalysts (denoted as Pd/SP-S-1 and Pd/SP-ZSM-5) through an incipient wetness impregnation strategy. Structural characterization by XRD and TEM demonstrates that the nanosheet zeolite frameworks are well preserved after metal incorporation, while Pd nanoparticles are uniformly distributed with a narrow size distribution centered at approximately 3.45 nm. XPS analysis indicates that Pd is mainly present in an oxidized Pd^{2+} state, together with a small proportion of Pd^{0} species. Benefiting from the nanosheet architecture and abundant anchoring sites, the prepared catalysts exhibit remarkable activity in methane combustion. Specifically, Pd/SP-S-1 delivers a T_{90} value of 459 °C, outperforming its counterpart supported on conventional S-1 zeolite. Further introduction of framework acidity leads to an additional enhancement in catalytic performance, decreasing the T_{90} of Pd/SP-ZSM-5 to 426 °C. Beyond activity, the acidic zeolite environment also contributes to improved durability, with Pd/SP-ZSM-5 sustaining stable methane conversion for nearly 50 h at 430 °C.

This study underscores the effectiveness of nanosheet zeolite supports in stabilizing active Pd species and illustrates a viable approach for constructing efficient methane combustion catalysts through the synergistic integration of metallic sites and acidic frameworks.

2 MATERIALS AND METHODS

2.1 Materials

Tetraethylorthosilicate (TEOS, Sinopharm Chemical Reagent Co., Ltd.), tetrabutylammonium hydroxide solution (TBAOH, 40 wt%, Aladdin), tetraethylammonium hydroxide (TEAOH, 25 wt%, Aladdin), aluminium isopropoxide ($\text{Al}(\text{O}i\text{Pr})_3$, Beijing Reagents Company), Sinopharm Chemical Reagent Co., Ltd.), sodium hydroxide (NaOH, 98%, Sinopharm Chemical Reagent Co., Ltd.), palladium chloride (PdCl_2 , Aladdin), ammonium chloride (NH_4Cl , Sinopharm Chemical Reagent Co., Ltd.).

2.2 Synthetic Methods

The defect-rich self-pillared silicalite-1 zeolite nanosheet (SP-S-1) was hydrothermally synthesized at 120 °C for 2 days using a molar composition of SiO_2 : TBAOH: H_2O = 1: 0.3: 10. In a typical procedure, 12.4 g of TBAOH solution was combined with 3.3 g of deionized water. Following 10 minutes of stirring, 12.48 g of TEOS was introduced, and the mixture was stirred continuously for 6 hours. The resulting clear solution was transferred into a 100 mL Teflon-lined stainless-steel autoclave and crystallized under static conditions at 120 °C for 2 days. The solid product was collected by centrifugation, washed repeatedly with water, dried at 80°C, and finally calcined in air at 550 °C for 6 hours to remove the organic template.

Defect-rich Self-pillared ZSM-5 zeolites (SP-ZSM-5) were synthesized under conditions similar to those for SP-S-1, with the addition of aluminum isopropoxide and sodium hydroxide to the synthesis gel. SP-ZSM-5-100 (Si/Al = 100) was prepared with a molar composition of SiO_2 : TBAOH: $\text{Al}(\text{O}i\text{Pr})_3$: H_2O = 1: 0.3: 0.01: 10, while SP-ZSM-5-50 (Si/Al = 50) was synthesized using SiO_2 : TBAOH: $\text{Al}(\text{O}i\text{Pr})_3$: NaOH: H_2O = 1: 0.3: 0.02: 0.02: 10.

Conventional nanosized silicalite-1 (S-1) was synthesized by first mixing 13 g of TPAOH solution with 15 g of deionized water under continuous stirring. After 10 minutes, 8.32 g of TEOS was added, and stirring was maintained for 6 hours. The clear solution, with a molar composition of SiO_2 : TPAOH: H_2O = 1: 0.4: 35, was transferred into a 100 mL Teflon-lined stainless-steel autoclave and crystallized at 170 °C for 3 days under static conditions. The solid product was then collected by centrifugation, washed with water several times, dried at 80 °C, and calcined at 550 °C for 6 hours to remove the organic template.

All the Pd-based catalysts were synthesized by an incipient wetness impregnation method. Typically, 200 mg calcinated SP-ZSM-5 or SP-S-1 was impregnated with 0.05 mL of aqueous $(\text{NH}_4)_2\text{PdCl}_4$ solution with certain concentrations. Then the sample was calcined in a muffle furnace at 500 °C for 6 hours.

2.3 Characterizations

The powder X-ray diffraction measurements were performed on a Rigaku D-Max 2550 diffractometer by using Cu $\text{K}\alpha$ radiation. The transmission electron microscopy measurements and energy dispersive X-ray spectra were taken with an FEI F200 Transmission electron microscope. CO pulse adsorption experiment was performed using an AMI-300 automated chemisorption analysis unit equipped with a thermal conductivity detector (TCD) under Ar flow. The performance evaluation device of the catalyst is a quartz fixed-bed reactor. Typically, 50 mg of catalyst (40-60 mesh) was mixed evenly with 200 mg of quartz sand (40-60 mesh), and then packed in a quartz tube (inner diameter: 6 mm, length: 350 mm). Both ends were fixed with quartz cotton. Methane gas (2% CH_4 -19.8% O_2 -78.2% N_2) was introduced, with a total gas flow rate of 30 $\text{mL}\cdot\text{min}^{-1}$, corresponding to a mass space velocity of 36,000 $\text{mL}\cdot\text{g}^{-1}\cdot\text{h}^{-1}$. The tail gas after the catalyst reaction was introduced into a gas chromatograph (FULI INSTRUMENTS GC-9790 plus) equipped with a flame ionization detector (FID) for online monitoring.

3 RESULTS AND DISCUSSION

3.1 Structure of the Catalyst

Figure 1 illustrates the synthetic procedure for immobilizing Pd nanoparticles within defect-rich self-pillared MFI nanosheets. Initially, self-pillared silicalite-1 (SP-S-1) and ZSM-5 (SP-ZSM-5) nanosheets are synthesized hydrothermally at 120 °C for two days using TBAOH as the structure-directing agent. Following synthesis, the materials are calcined in air at 550 °C for six hours to remove the organic template. Subsequently, Pd nanoparticles are introduced into the MFI zeolite nanosheets via impregnation with an $(\text{NH}_4)_2\text{PdCl}_4$ solution, after which the samples are calcined at 500 °C for another six hours in a muffle furnace. The resulting catalysts are designated as Pd/SP-S-1, Pd/SP-ZSM-5-100, and Pd/SP-ZSM-5-50, where the numerical suffixes indicate the Si/Al molar ratios of the respective zeolite supports.

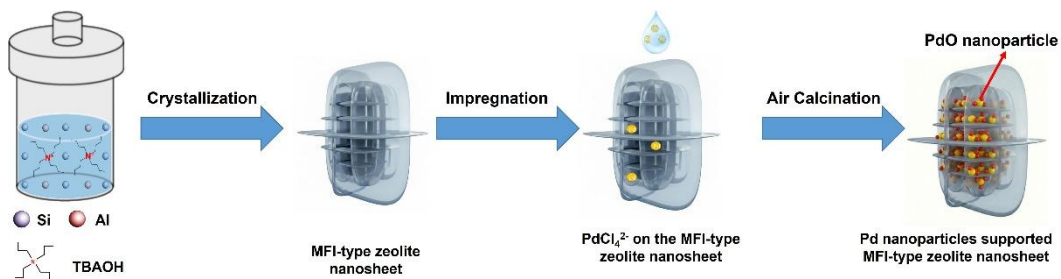


Figure 1 The Schematic for Pd Nanoparticles Supported MFI-type Zeolite Nanosheet

Powder X-ray diffraction (PXRD) patterns confirm that all metal-containing samples preserve the characteristic diffraction features of the MFI framework, with no additional reflections attributable to crystalline metallic phases detected within the resolution limit of the technique (Figure 2). This observation indicates that the introduction of metal species does not induce any detectable structural degradation or phase transformation of the zeolite framework, and further suggests that the metal nanoparticles are highly dispersed and/or present in an amorphous or ultrafine state. The retention of the MFI topology after metal incorporation highlights the structural robustness of the nanosheet zeolite supports and their suitability for stabilizing metal species. To gain deeper insight into the surface chemical states of the supported metal species and to probe possible electronic interactions between the metal nanoparticles and the zeolite support, X-ray photoelectron spectroscopy (XPS) measurements were performed. The Pd 3d core-level spectra of Pd nanoparticles supported on MFI-type zeolite nanosheets display two dominant peaks at binding energies of 336.3 eV and 337.8 eV, which can be assigned to the Pd 3d_{5/2} and Pd 3d_{3/2} components, respectively. These binding energy values are characteristic of Pd²⁺ species, indicating that palladium is predominantly present in an oxidized PdO-like state on the zeolite nanosheets. In addition to the dominant Pd²⁺ contribution, a weak shoulder at lower binding energy can be discerned, corresponding to a minor fraction of metallic Pd⁰ species.

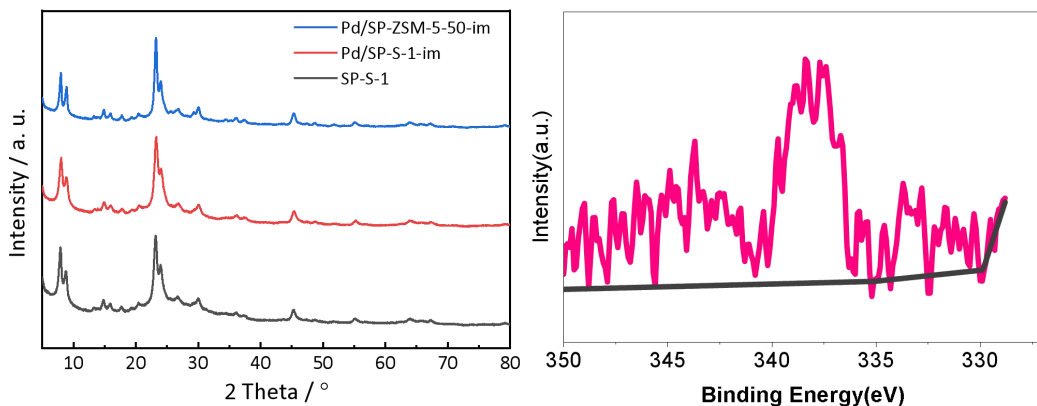


Figure 2 The XRD Patterns and XPS Spectra for Pd Nanoparticles Supported MFI-type Zeolite

High-resolution scanning transmission electron microscopy (STEM) and transmission electron microscopy (TEM) images of the Pd-loaded MFI zeolites are presented in Figures 3 and 4. The SP-S-1 zeolite displays a self-pillared nanosheet morphology, with individual lamellae measuring less than 10 nm in thickness. Introducing more Al atoms into the zeolite framework slightly increases the crystal size, yet the average thickness of SP-ZSM-5 nanosheets remains around 20 nm. Pd nanoparticles in Pd/SP-S-1 are uniformly distributed throughout the zeolite matrix, with an average size of approximately 3.45 nm. Similarly, Pd nanoparticles in Pd/SP-ZSM-5-50 also exhibit an average size of about 2.72 nm, indicating that the introduction of Brønsted acid sites does not significantly affect nanoparticle formation. Moreover, the observed lattice spacing of 0.28 nm corresponds to the typical structure of PdO, which aligns consistently with the XPS results.

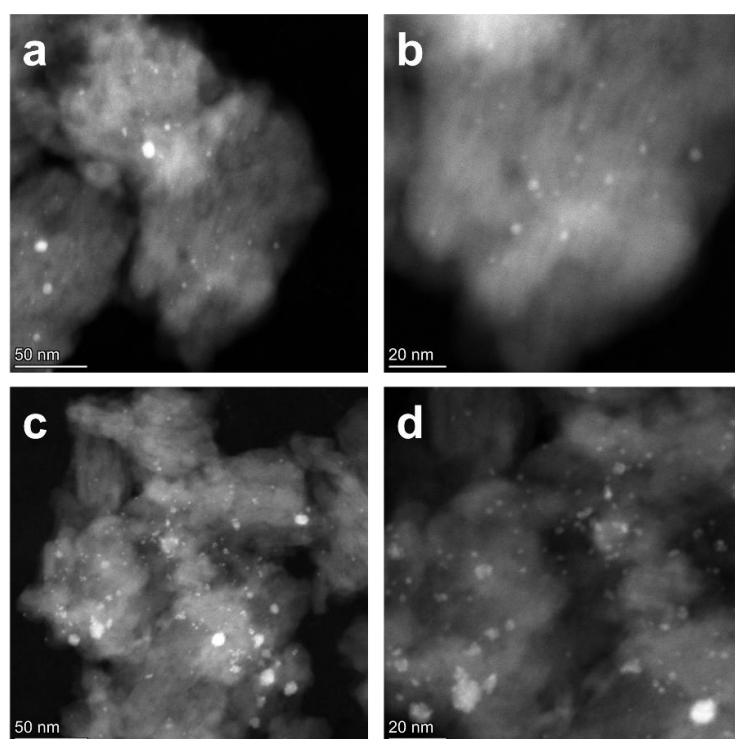


Figure 3 High Resolution STEM Images of Pd/SP-S-1 Catalyst

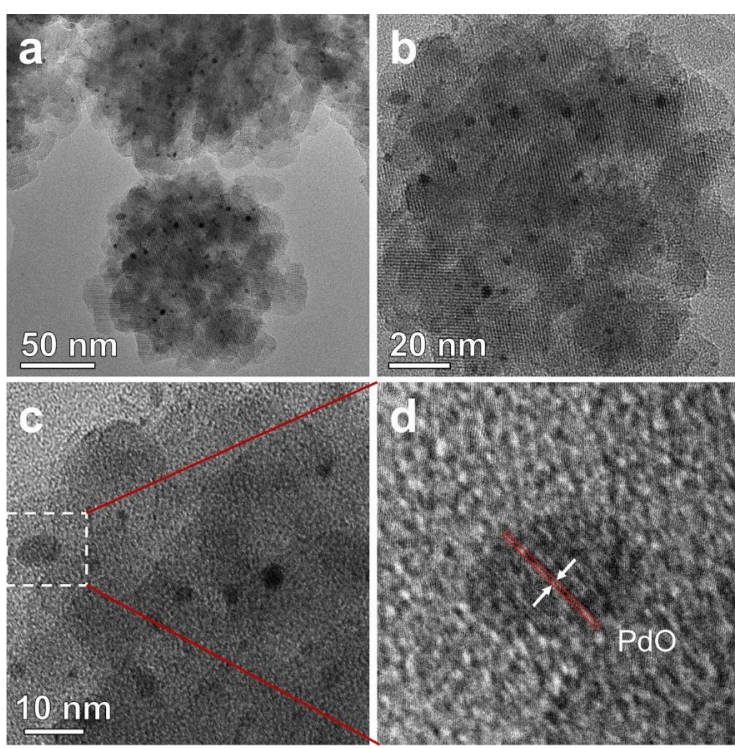


Figure 4 High Resolution TEM Images of Pd/SP-ZSM-5 Catalyst

3.2 Catalytic Performances

The catalytic performance for complete methane combustion is initially evaluated under a gas hourly space velocity (GHSV) of $36,000 \text{ mL} \cdot \text{g}_{\text{cat}}^{-1} \cdot \text{h}^{-1}$ and a reactant mixture consisting of 2%CH₄, 19.8%O₂ and 78.2%N₂. As shown in Figure 5a, methane conversion increases with rising reaction temperature for all catalysts. Pd/SP-S-1 demonstrates high catalytic activity, with T₅₀ and T₉₀ values (temperatures required for 50% and 90% methane conversion, respectively) of 398 °C and 459 °C (Figure 5c). In contrast, Pd/S-1 exhibits significantly lower activity, with T₅₀ and T₉₀ values of 527 °C and 556 °C, likely due to the poor metal dispersion associated with conventional zeolite supports as shown in the CO pulse adsorption results (Figure 5d). Notably, Pd/SP-ZSM-5, which incorporates Brønsted acid sites, shows even lower T₅₀ (382 °C) and T₉₀ (426 °C), indicating superior catalytic activity. Given the comparable nanoparticle sizes in Pd/SP-S-1

and Pd/SP-ZSM-5, the enhanced performance of Pd/SP-ZSM-5 is attributed to the synergistic interaction between palladium nanoparticles and the zeolite acid sites [11].

Catalyst durability, which is a key requirement for practical methane combustion applications, was evaluated by time-on-stream (TOS) measurements under dry reaction conditions at 430 °C, as shown in Figure 5b. The Pd@DeAl-Beta-SEA catalyst exhibits a gradual loss of activity, with methane conversion decreasing from approximately 83% to 70% over 50 h of continuous operation, indicating progressive deactivation. In sharp contrast, the Pd/SP-ZSM-5 catalyst displays markedly enhanced stability. Owing to the presence of Brønsted acid sites, Pd/SP-ZSM-5 maintains a nearly constant CH₄ conversion of ~93% for more than 100 h on stream, demonstrating its excellent long-term operational stability. Catalyst durability, a critical factor for practical application, is assessed through time-on-stream (TOS) testing under dry conditions at 430 °C (Figure 5b).

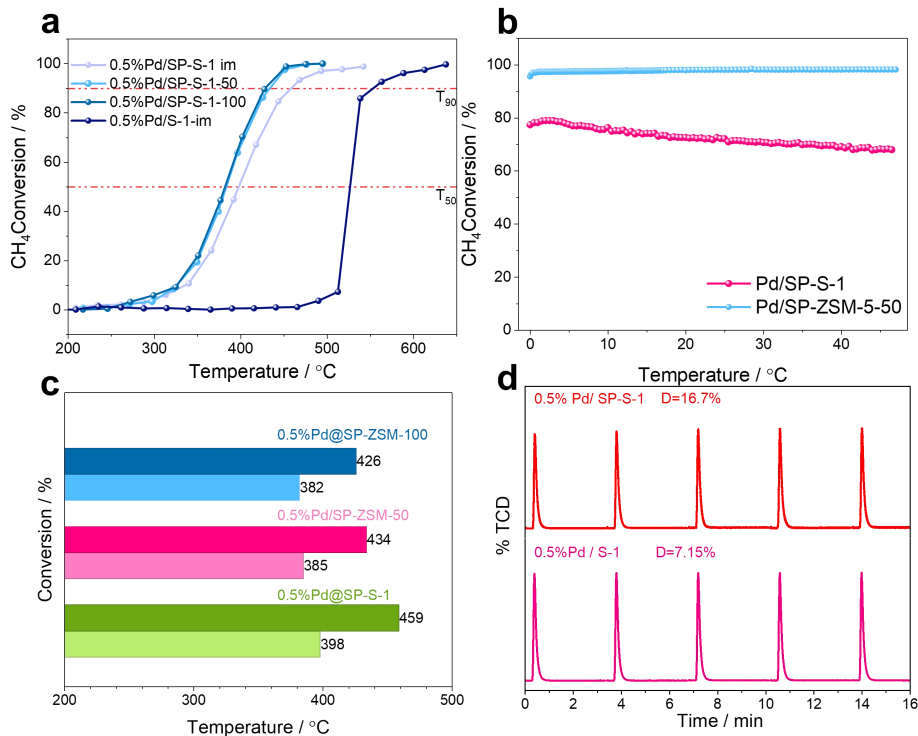


Figure 5 Catalytic Performance of MFI Zeolite Supported Pd Catalysts for CH₄ Combustion: (a) Light-off Curves; (b) Long-Term Stability in Dry Conditions; (c) T50 and T90 Values; (d) CO Pulse Adsorption Results

Post-reaction characterization further elucidates the stability of the catalysts. The Pd 3d XPS spectra (Figure 6a) confirm that Pd species in the spent catalyst remain predominantly in the PdO state, with binding energies of 336.8 eV (Pd 3d_{5/2}) and 338.1 eV (Pd 3d_{3/2}). TEM analysis (Figure 6b) reveals that the metal cluster size and zeolite morphology in Pd/SP-ZSM-5 are virtually unchanged after reaction, with no significant nanoparticle aggregation observed. These results collectively demonstrate the exceptional stability of Pd nanoparticles supported on MFI-type zeolite nanosheets for methane combustion.

The Pd 3d XPS spectra show that the catalyst after reaction is still predominantly composed of PdO species, exhibiting binding energies of 336.8 eV for Pd 3d_{5/2} and 338.1 eV for Pd 3d_{3/2} (Figure 6a). Significantly, the size of metal clusters and the morphology of zeolite for the Pd/SP-ZSM-5 catalyst remain identical with the fresh one based on the TEM measurements (Figure 6b). No severe aggregation of metal nanoparticles can be observed for the Pd/SP-ZSM-5 catalyst. The above results further reveal excellent stability of Pd nanoparticles supported MFI-type zeolite nanosheet for CH₄ combustion.

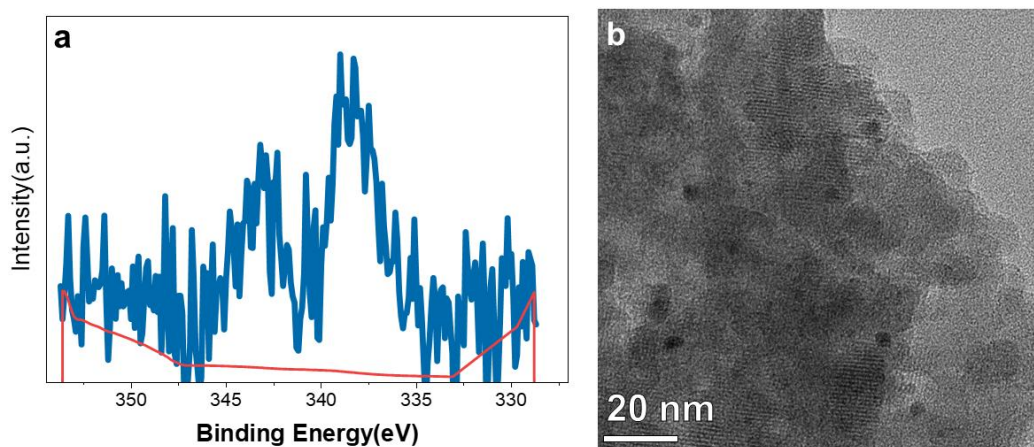


Figure 6 XPS spectra and TEM image of Pd/SP-ZSM-5 Catalyst after Long-Term Stability Test

4 CONCLUSION

Catalytic methane combustion is crucial for mitigating environmental impacts, as palladium nanoparticles serve as highly active catalysts but tend to aggregate due to their high surface energy. In this study, defect-rich MFI-type zeolite nanosheets (SP-S-1 and SP-ZSM-5) are employed as supports to immobilize Pd nanoparticles via incipient wetness impregnation. The resulting catalysts exhibit excellent methane combustion activity. The T_{90} of Pd/SP-S-1 is 459 °C, outperforming the conventional S-1-supported counterpart. Introducing acidity further enhances catalytic performance, lowering the T_{90} of Pd/SP-ZSM-5 to 426 °C. Moreover, the acidic zeolite framework improves Pd stability, with Pd/SP-ZSM-5 maintaining steady activity for nearly 50 hours at 430 °C. This work demonstrates the potential of nanosheet zeolite-stabilized Pd catalysts for efficient methane combustion through synergistic metal-acid interactions.

COMPETING INTERESTS

The authors have no relevant financial or non-financial interests to disclose.

ACKNOWLEDGEMENTS

The authors thank the support by the start-up supports from Qingdao University.

REFERENCES

- [1] Choudhary TV, Banerjee S, Choudhary VR. *Applied Catalysis A: General*. 2002, 234: 1-23.
- [2] He L, Fan Y, Bellettre J, et al. *Renewable and Sustainable Energy Reviews*. 2020, 119: 109589.
- [3] Zhang C, Chen X, Zhang S, et al. *Journal of Materials Chemistry A*. 2025.
- [4] Li T, Beck A, Krumeich F, et al. *ACS Catalysis*. 2021, 11: 7371-7382.
- [5] Chen H Y, Lu J, Fedeyko J M, Raj A. *Applied Catalysis A: General*. 2022, 633: 118534.
- [6] Wang W, Zhou W, Li W, et al. *Applied Catalysis B: Environment*. 2020, 276: 119142.
- [7] Wang N, Sun Q, Bai R, et al. *Journal of the American Chemical Society*. 2016, 138: 7484-7487.
- [8] Ryoo R, Kim J, Jo C, et al. *Nature*. 2020, 585: 221-224.
- [9] Zhang Y, Yan Z, Xiao M, et al. *Journal of Environmental Sciences*. 2025, 152: 248-261.
- [10] Li A, Zhang Y, Heard C J, et al. *Angewandte Chemie International Edition*. 2023, 62: e202213361.
- [11] Wang Y, Shen G, Xiong W, et al. *Applied Catalysis A: General*. 2023, 665: 119358.